Science Advances
AAAS

Supplementary Materials for

Spontaneous beat synchronization in rats: Neural dynamics and motor entrainment

Yoshiki Ito *et al.*

Corresponding author: Hirokazu Takahashi, takahashi@i.u-tokyo.ac.jp

Sci. Adv. **8**, eabo7019 (2022)
DOI: 10.1126/sciadv.abo7019

The PDF file includes:

Figs. S1 to S12
Legends for movies S1 to S3

Other Supplementary Material for this manuscript includes the following:

Movies S1 to S3

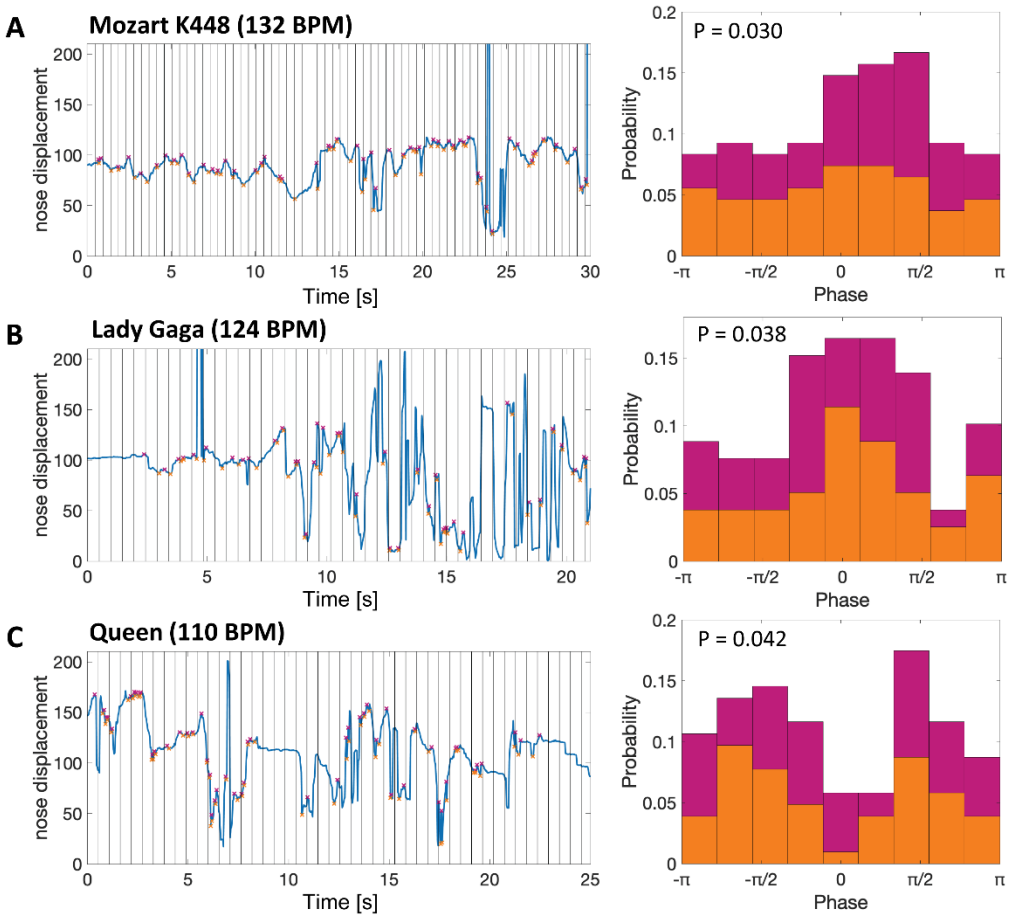

Fig. S1. Visually characterized beat synchronous movement in a biped stance. (**A**) (Left) Nose displacement calculated from the result of DeepLabCutTM (*63*) during presentation of Mozart K.448 (see Movie S2). The upper and lower peaks were detected. (Right) Histogram of detected peaks in the phase space. Magenta depicts upper peaks and orange lower peaks. The peak around 0º was observed with statistically significantly non-uniformity (Rayleigh's test). (**B**) Lady Gaga, "Born this way" (Movie S2). (**C**) Queen, "Another one bite the dust" (Movie S2). Because of the bimodal distribution in Queen condition, the phase was doubled in Rayleigh's test.

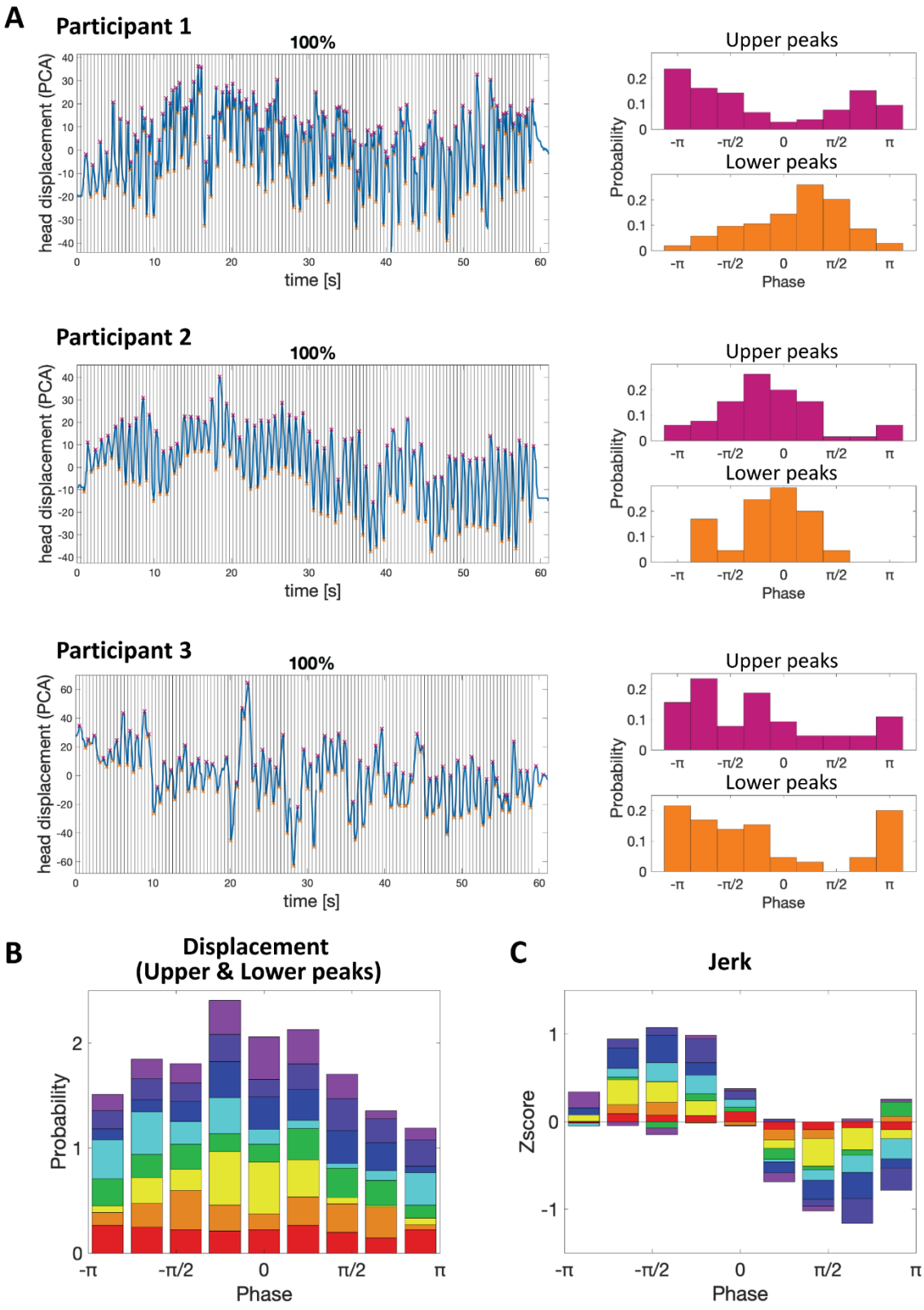

Fig. S2. Inter-subject variability of beat synchronization in humans. (**A**) Representative head displacement during the presentation of Mozart K. 448. (Left) The

first component of the principal component analysis of visually detected two-dimensional head displacement was plotted across the musical passage. The upper and lower peaks of head displacement at the original tempo were detected and marked in magenta and orange respectively. (Right) Histograms of angle exhibiting the upper and lower peaks. The timing of beat was at phase 0. Three representative participants were plotted. The characteristics of the histogram indicated that each participant synchronized to the beat differently (see Movie S3): The upper and lower peaks appeared around π and 0 in Participant 1, 0 and 0 in Participant 2, and π and π in Participant 3. (**B**) Summary of head displacement. The probability histogram in each subject was stacked in a bar. Each participant (n = 8) was plotted in different colors. (**C**) Head movement characterized by the head jerk. Z-score in each subject was stacked in a bar. The jerk was consistently maximized around $-\pi/2$ and minimized around $\pi/2$ in most subjects, suggesting that the head jerk movement was a reliable measure of beat synchronization.

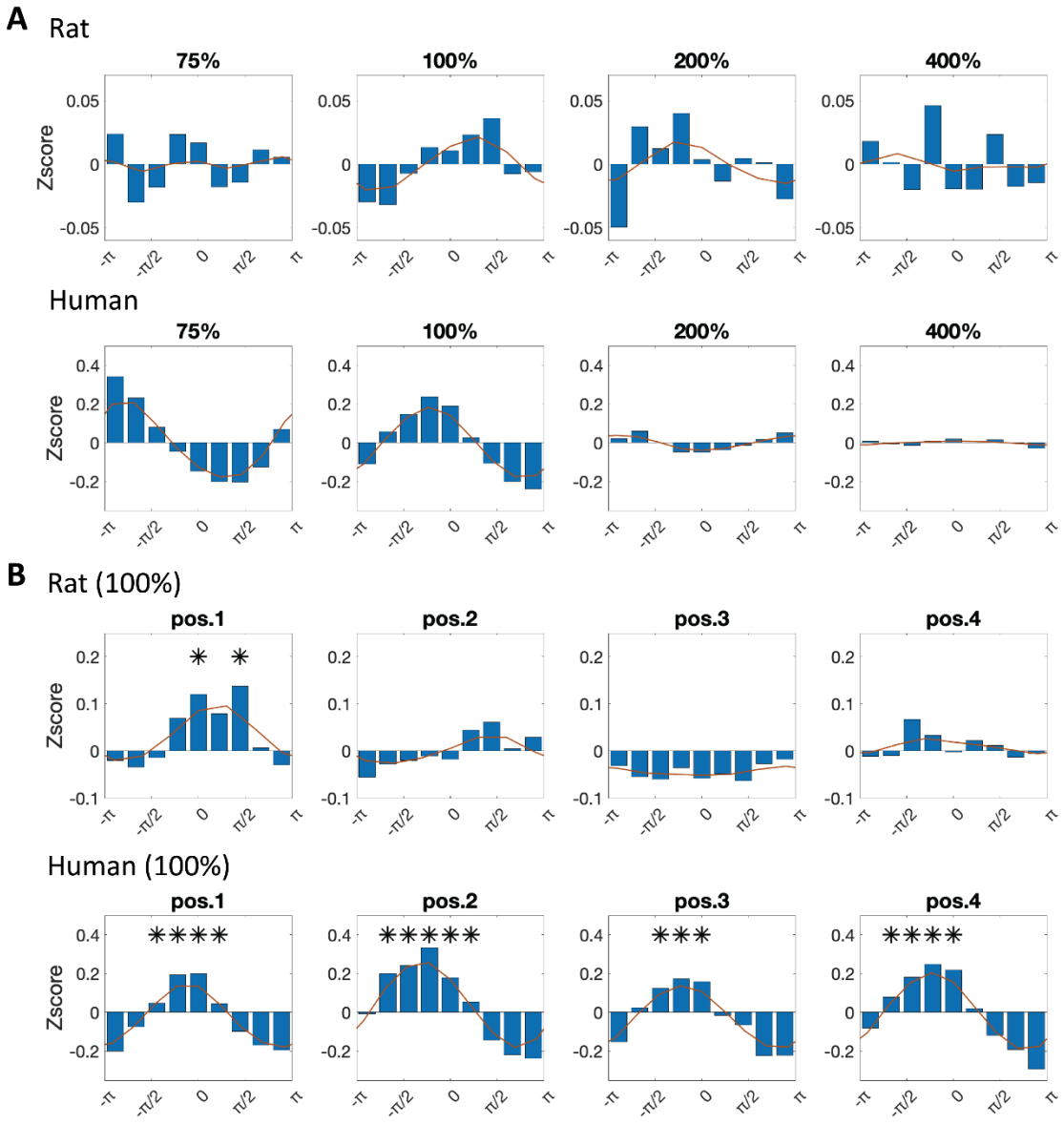

Fig. S3. Jerk as a function of the phase angle between metric positions of beats. (**A**) Z-score of mean jerk at each angle were plotted at each playback tempo (75%, 100%, 200% and 400%). The timing of the beat was at phase 0. The Z-scores were averaged among subjects exhibiting a significant beat contrast at the original tempo (n = 5 in rats, and n = 12 in humans). For visualization purpose, weighted Gaussian kernel density function was estimated and depicted in red lines. (**B**) Z-scores of mean jerk at the original tempo (100%) were plotted at each metric position of the beats (Fig. 3A). Asterisks indicate that the jerk was significantly positive (one-sided t-test, $P < 0.05$).

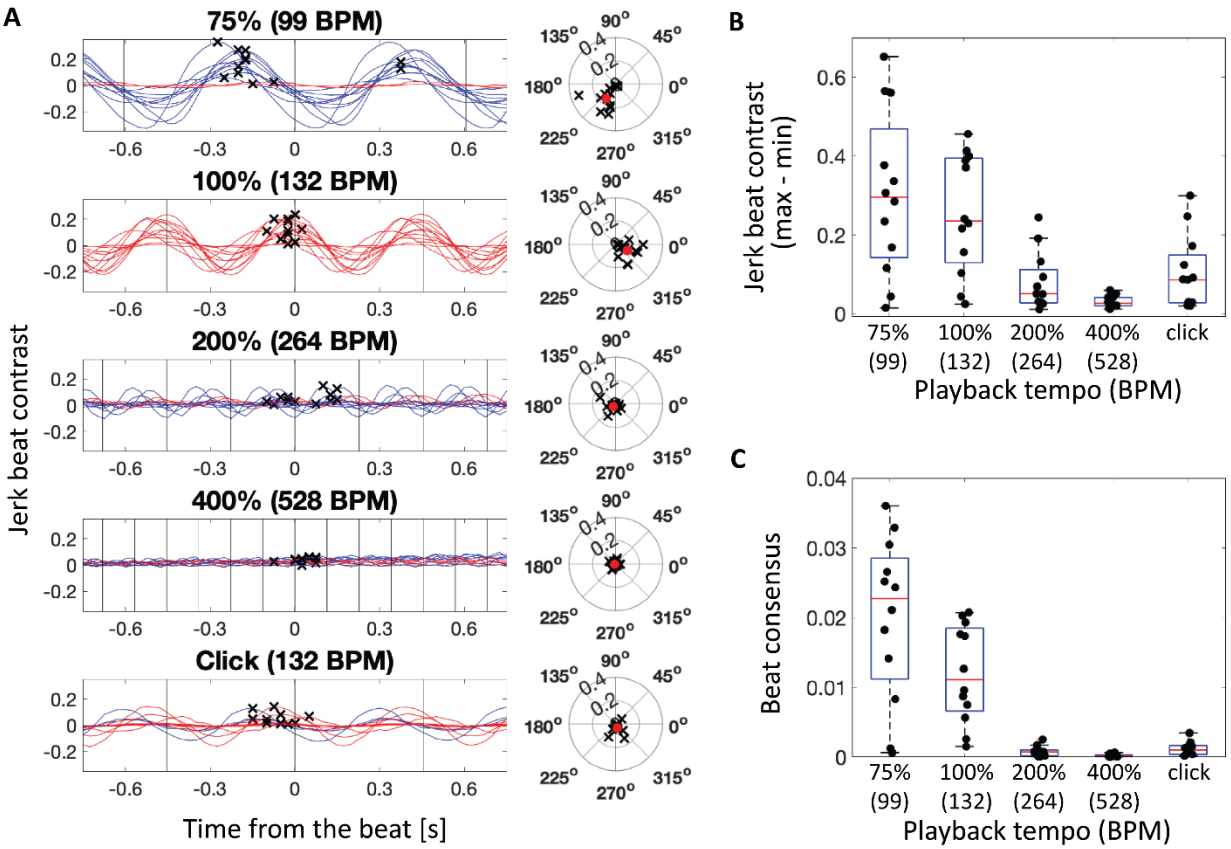

Fig. S4. Beat synchronization movements in humans. (**A**) (Left) Mean jerk beat contrast values are calculated by shifting the window of the putative on-beat timing for each tempo. Click (132 BPM) indicates a click sequence of rasterized rhythm of the original piece. In-phase synchrony is plotted in red, whereas reverse-phase synchrony is plotted in blue. The crosses indicate the maximum jerk beat contrast in a cycle (n = 12). (Right) Distribution of maximum jerk beat contrast plotted in the phase field with 0° corresponding to a beat. Each cross indicates a subject, and the red dot indicates the average. (**B**) Amplitude of jerk beat contrast variation (max–min) in each playback tempo. Each black dot indicates a subject. (**C**) Inter-subject similarity of beat contrast defined as beat consensus. See Fig. 1 for conventions.

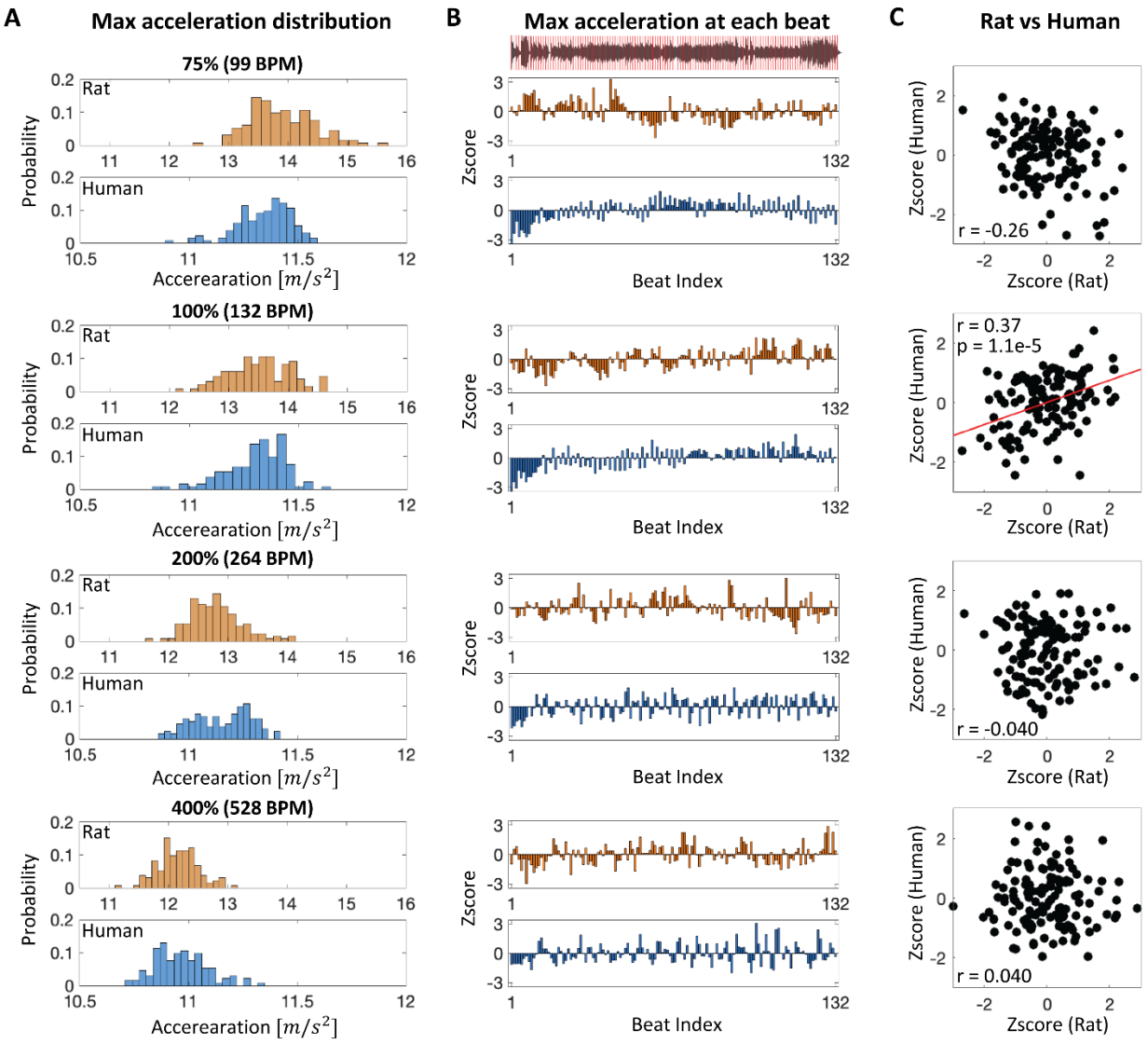

Fig. S5. Comparison of beat synchronization in acceleration between rats and humans during music presentation (K. 448). (**A**) Distribution of maximum acceleration between each beat as a function of playback tempos (75, 100, 200 and 400%). (**B**) Maximum acceleration at each beat. Z-scores of acceleration plotted at each beat index (#1–#132). (**C**) Correlation of acceleration at each beat index between rats and humans. The correlation coefficient (r) is indicated in each inset.

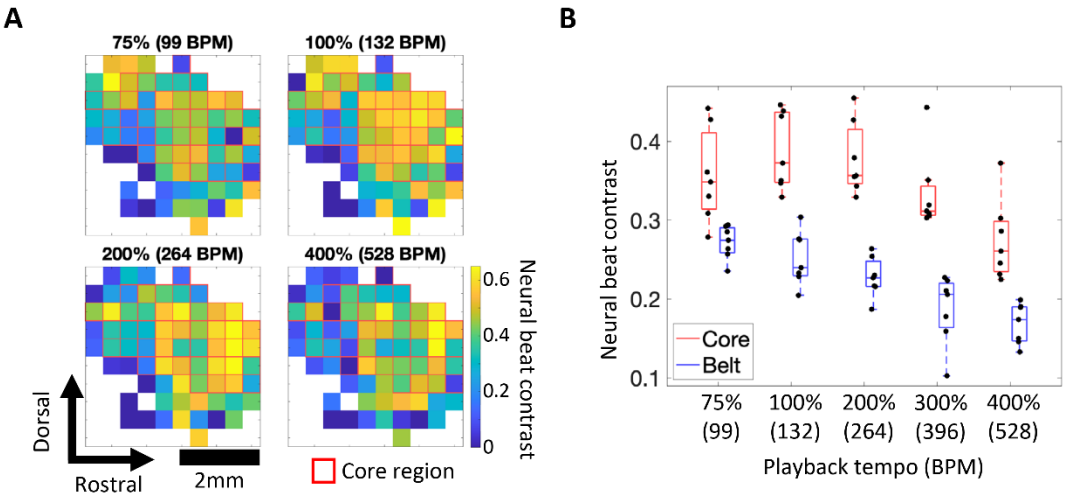

Fig. S6. Regional differences of neural beat contrast. (**A**) Spatial distribution of neural beat contrast in the auditory cortex of a representative animal. Color-mapped neural beat contrast of all recording sites in auditory cortex. Each square represents an electrode. Red outlined squares are located in the core region, while others are in the belt region. (**B**) MUA beat contrast as a function of playback tempo. The mean neural beat contrasts across test rats in either the core or belt region are represented. Each black dot indicates an animal.

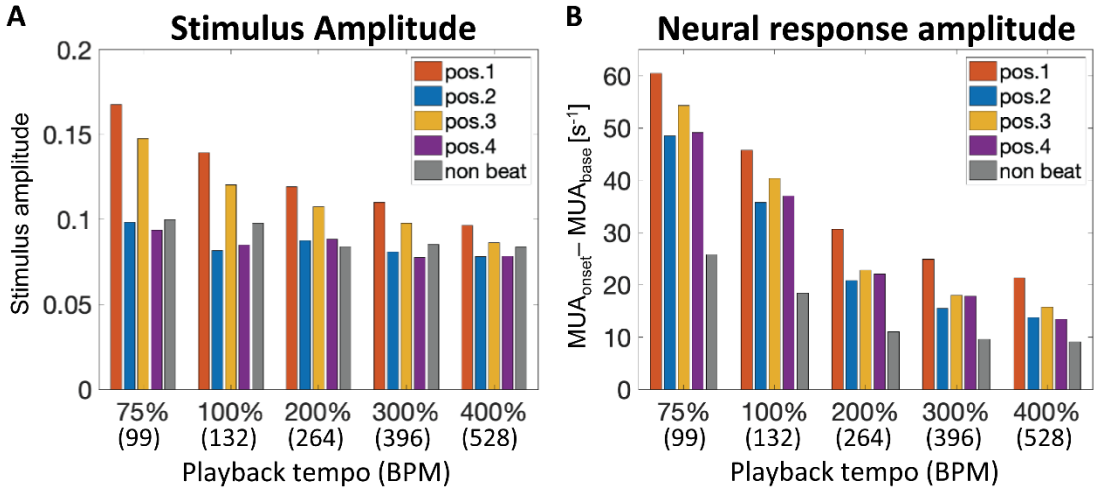

Fig. S7. Stimulus amplitude and neural responses as a function of metric position of beats in music. (**A**) The mean amplitude of the beat was quantified from the music stimulus data (WAV file) used in the experiment. (**B**) The neural response was quantified as the difference between MUA_{onset} and MUA_{base}. While the beat notes at pos.2 and pos.4 were as large as non-beat notes, the neural responses to non-beat sound were smaller than those of pos.2 (P = 2.6e-2) and pos.4 (P = 7.0e-3) (Mann–Whitney U test), suggesting that the acoustic energy did not purely reflect the neural response magnitudes.

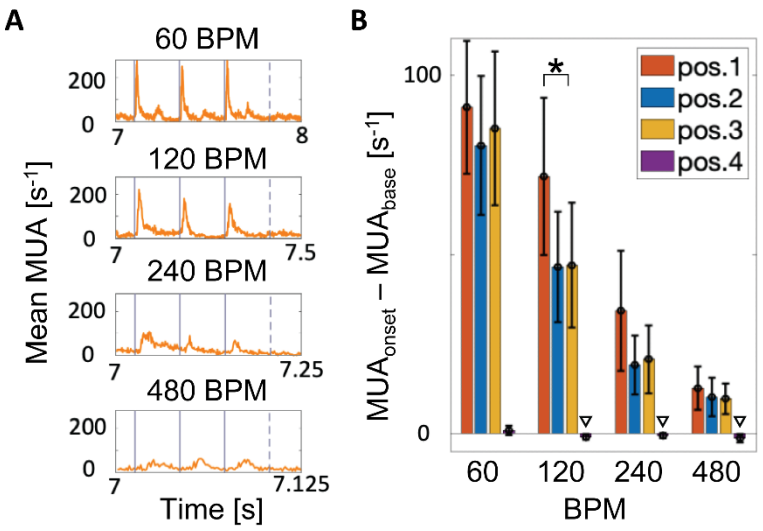

Fig. S8. Evoked MUAs in a rhythmic click sequence as a function of metric position. (**A**) MUA transients within a rhythmic sequence cycle were averaged across trials in a representative subject. Each stimulus consisted of 3 consecutive clicks (solid lines) followed by a rest (broken line). (**B**) The neural response was quantified as the difference between MUA_{onset} and MUA_{base}. Asterisks indicate significant differences between metric positions (Kruskal-Wallis test, $P = 0.032$). Inverted triangles indicate that the neural response was significantly negative (one-sided t-test, $P = 1.7e\text{-}3$, $1.9e\text{-}2$ and $3.2e\text{-}3$, for 120, 240 and 480 BPM, respectively).

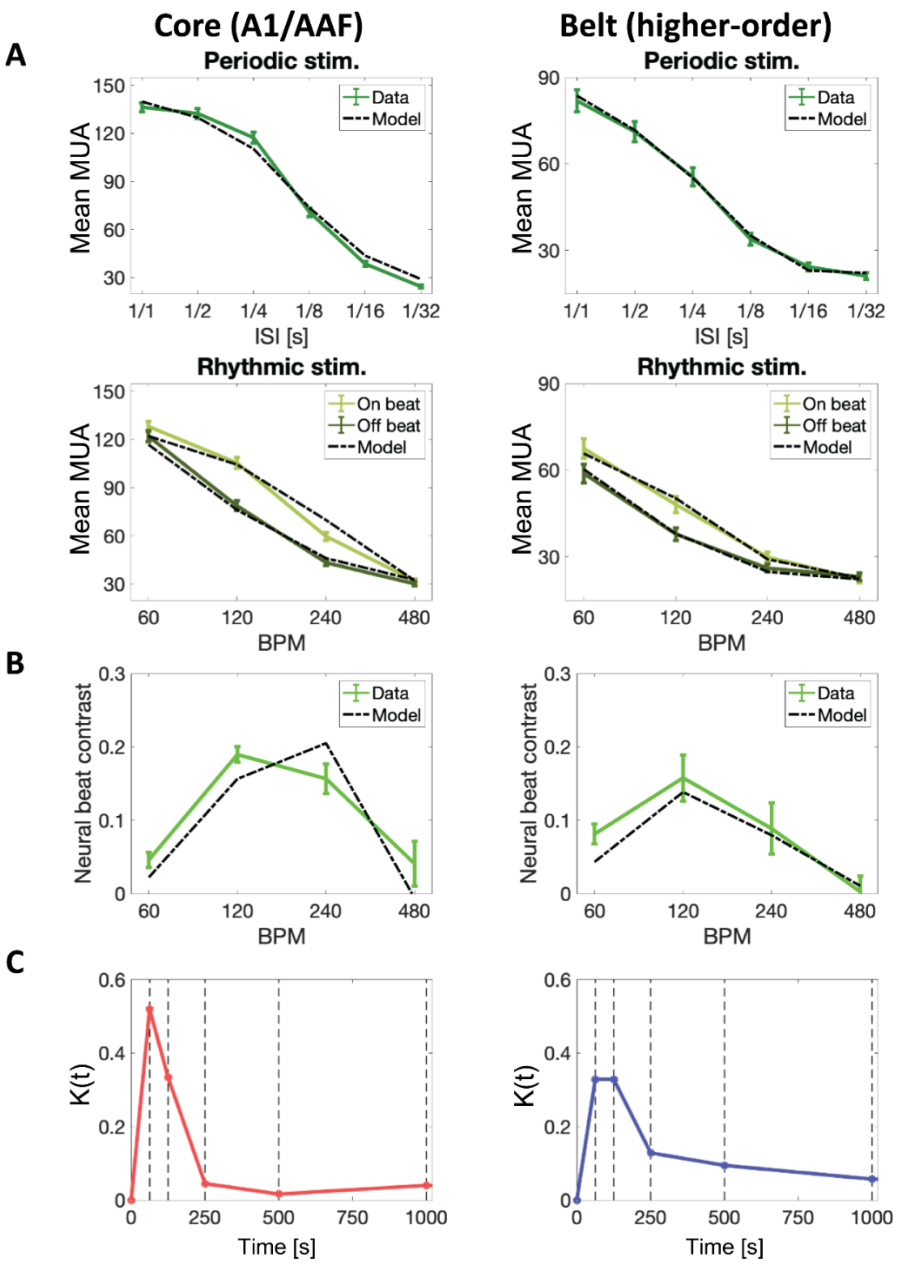

Fig. S9. Regional differences in short-term adaptation in the auditory cortex. (**A**) Mean MUA response to the periodic click sequence (Top) and the rhythmic click sequence (Bottom), in either the core cortex (the primary and anterior auditory fields) (Left) or in the belt cortex (higher-order auditory fields) (Right). Solid lines indicate MUAs in electrophysiological experiments, and dashed lines indicate the simulation results. The error bar indicates the standard error of the mean. (**B**) Simulation of the neural beat contrast in the rhythmic click sequences. The neural beat contrast of the belt was maximized around 120 BPM, suggesting that short-term adaptation in the higher-order auditory cortex is crucial for beat tuning. (**C**) The outline of kernel function in each region. The short-term adaptation in the core was effective only for 250 ms, while that in the belt lasted for 500 ms and was close to the inter-stimulus interval of 120 BPM.

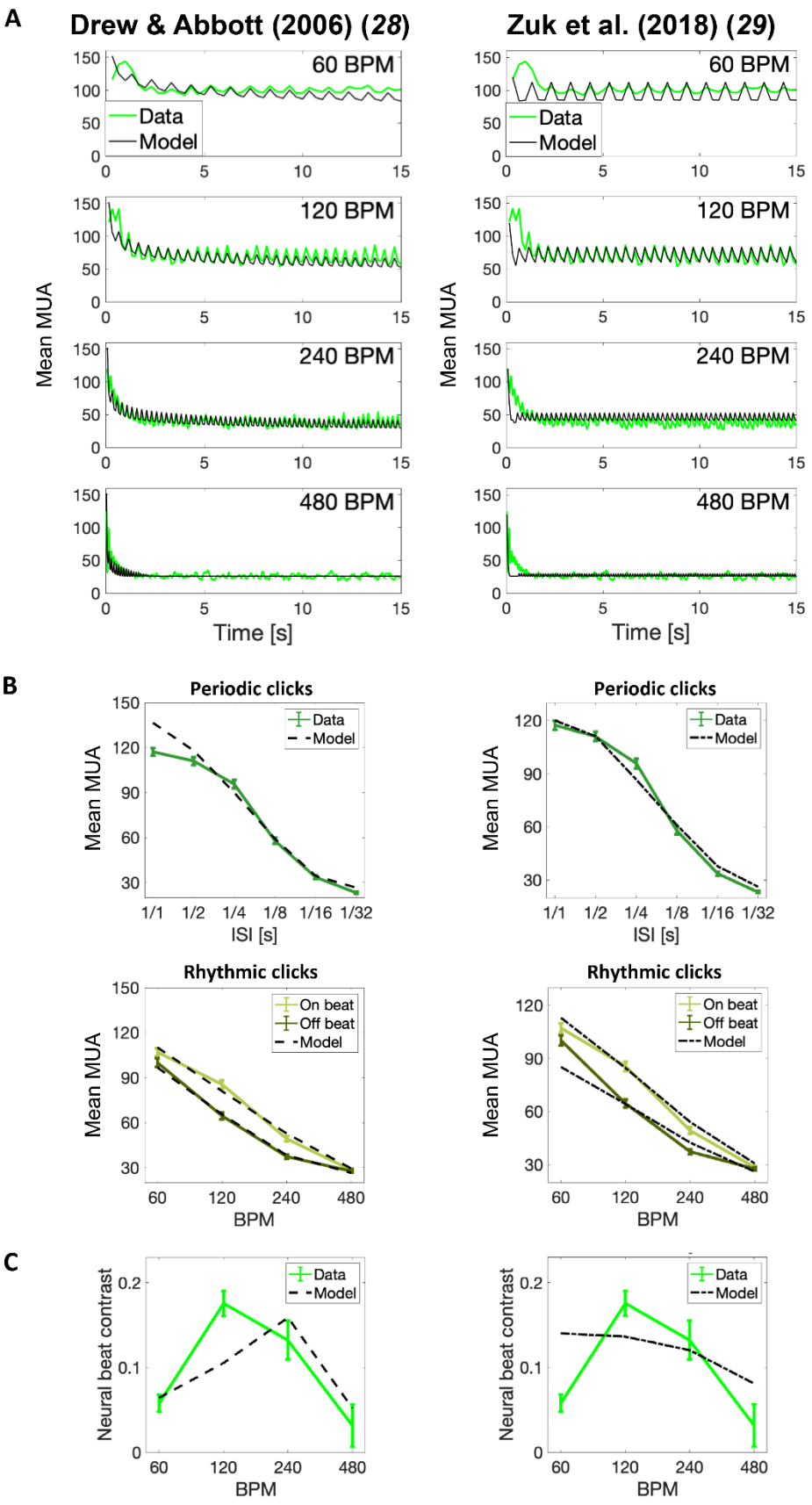
A
Drew & Abbott (2006) (28)
Zuk et al. (2018) (29)
60 BPM
120 BPM
240 BPM
480 BPM
Data
Model
Mean MUA
Time [s]
B
Periodic clicks
Rhythmic clicks
On beat
Off beat
ISI [s]
BPM
C
Neural beat contrast

Fig. S10. Simulation of MUA responses by existing models. (**A**) MUA responses to the rhythmic click sequence were simulated by adaptation models from Drew & Abbott (2006) (*28*) (Left) and Zuk et al. (2018) (*29*) (Right). Green lines indicate the mean of click-evoked MUA among all test recording sites in electrophysiological experiments, and black lines indicate simulation results. (**B**) Mean MUA response to the periodic click sequence (Top) and the rhythmic click sequence (Bottom). Solid lines indicate MUAs in electrophysiological experiments, and dashed lines indicate the simulation results. The error bar indicates the standard error of the mean. Both models were unable to explain both periodic and rhythmic conditions with the same parameters. (**C**) Simulation of neural beat contrast in the rhythmic click sequences. The peak in the simulation with conventional models deviated from the empirical data. The outline of kernel function used in this simulation is shown in Fig. 4G.

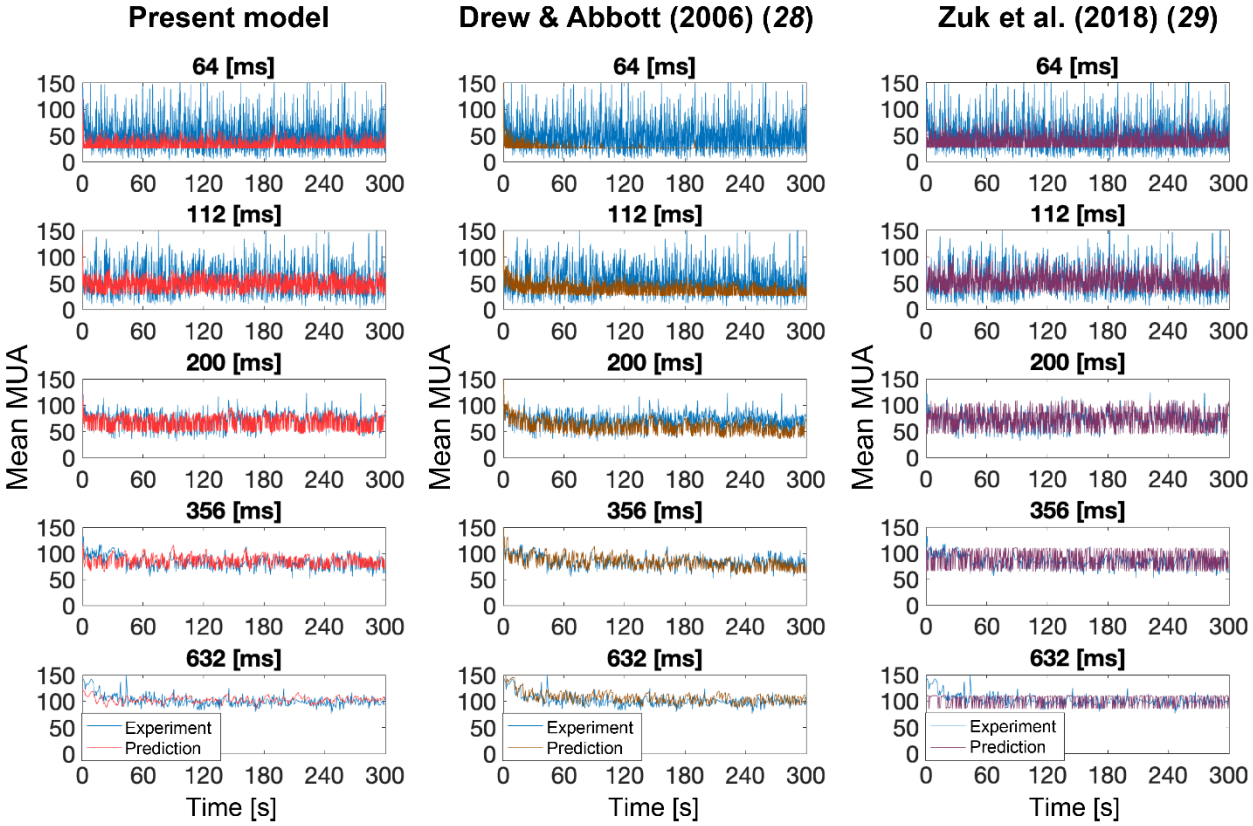

Fig. S11. Model comparison of neural activity prediction to random click sequence. Prediction of MUA response to random click sequences by the present work (Left), Drew & Abbott (2006) (*28*) (Middle), and Zuk et. al. (2018) (*29*) (Right). Blue lines show the experimental results and other color lines show the prediction results. The mean ISI of random click sequences is indicated at the top of each inset. The outline of kernel functions and the representative MUA used in the simulation are shown in Fig. 4G and H, respectively.

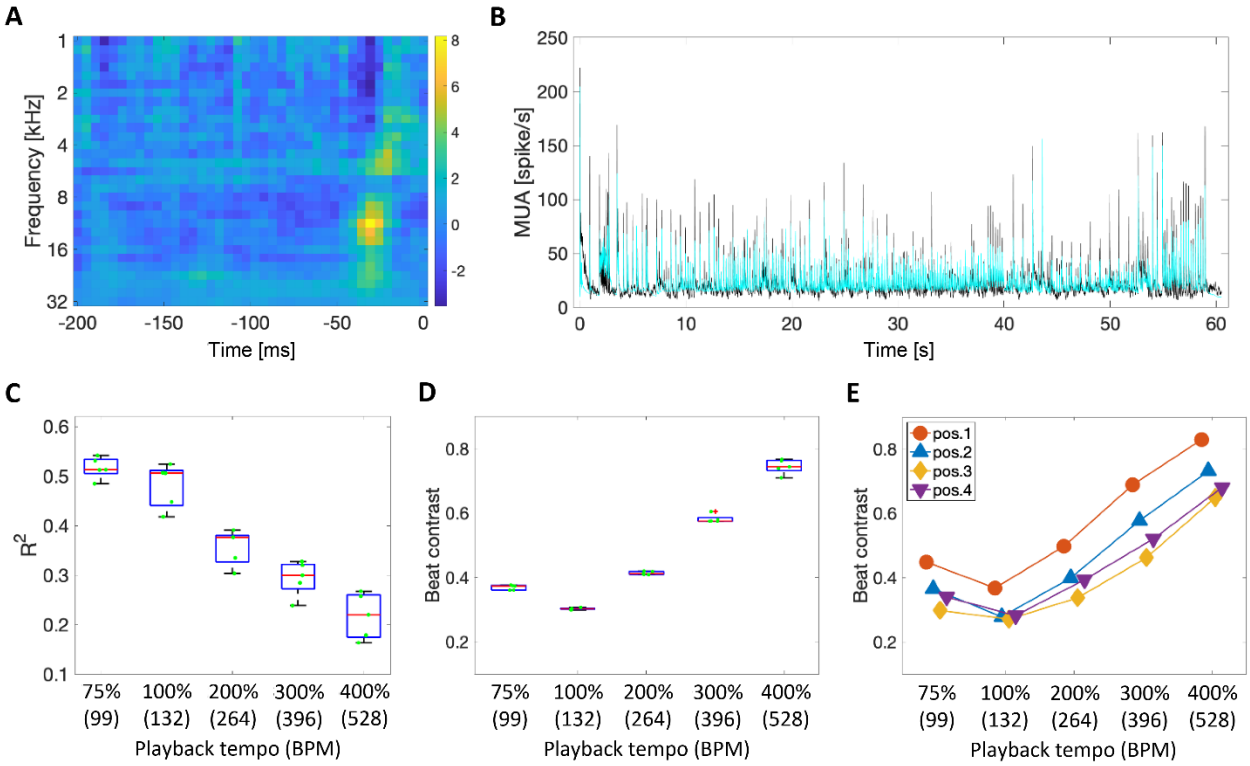

Fig. S12. Spectrotemporal receptive field (STRF) cannot explain the neural tuning within 120-140 BPM. (**A**) STRF was calculated based on previous literature (*20, 30*). (**B**) Representative fitting result of MUA at the playback tempo of the original tempo by the STRF based linear-nonlinear model. (**C**) The fitting accuracy (R^2) at each playback tempo. The fitting accuracy decreased with playback tempo. (**D**) Prediction of neural beat contrast averaged among beat positions (experimental data in Fig.3C). (**E**) Prediction of neural beat contrast at each beat position (experimental data in Fig.3D). The local maximum around original playback tempo cannot be explained by this STRF model.

Movie S1. Rat movements during music presentation. The slow-motion playback in the latter half caused the change in pitch.

Movie S2. Visually characterized beat synchronous movement in a biped stance. (**A**) Mozart, K.448; (**B**) Lady Gaga, Born this way; and (**C**) Queen, Another one bite the dust.

Movie S3. The head movement of human subjects during music presentation. Mozart K. 448 at the original tempo was presented. The head displacements in the movies were extracted and shown in Fig. S2 (Participants 1-3).